Cellular automaton model for diffusive and dissipative systems

T. C. Chan,[1] H. F. Chau,[2,3]* and K. S. Cheng[1]
[1]*Department of Physics, University of Hong Kong, Pokfulam Road, Hong Kong*
[2]*School of Natural Sciences, Institute for Advanced Study, Olden Lane, Princeton, New Jersey 08540*
[3]*Department of Physics, University of Illinois, 1110 West Green Street, Urbana, Illinois 61801*
(Received 4 October 1994)

We study a cellular automaton model which allows diffusion of energy (or equivalently any other physical quantities such as mass of a particular compound) at every lattice site after each time step. A unit amount of energy is randomly added onto a site. Whenever the local energy content of a site reaches a fixed threshold E_{c1}, energy will be dissipated. The dissipation of energy propagates to the neighboring sites provided that the energy contents of those sites are greater than or equal to another fixed threshold E_{c2} ($\leq E_{c1}$). Under such dynamics, the system evolves into three different types of states depending on the values of E_{c1} and E_{c2} as reflected in their dissipation size distributions, namely, localized peaks, power laws, or exponential laws. This model is able to describe the behaviors of various physical systems including the statistics of burst sizes and burst rates in type-I x-ray bursters. Comparisons between our model and the famous forest-fire model are made.

PACS number(s): 05.40.+j, 05.70.Fh, 05.70.Ln, 64.60.−i

I. INTRODUCTION

For many years, cellular automaton models have been playing important roles in the study of nonlinear and spatially extended systems. In most cases, these models cannot be solved analytically and their investigations rely mainly on computer simulations. The forest-fire model (FFM) [1], the Eden model [2], and earthquake simulations [3] are some examples. Besides, many simplifications have been made in these models, making their underlying physics unclear. In this paper, we introduce a simple cellular automaton model that accounts for the stochastic energy (or equivalently any other physical quantity) introduction, occasional energy dissipation, and energy diffusion in an open physical system. This kind of nonequilibrium system is common in nature. We find that the system shows different behaviors with different parameters. With an appropriate choice of parameters, the model can be applied (sometimes after small changes in the geometry) to explain the statistics of the occasional outburst of energy (or other physical quantities) in various physical systems including the thermonuclear runaways in x-ray bursters [4] and the sudden CO_2 gas release in crater lakes [5].

We introduce the model in Sec. II. Then we discuss the significance of various parameters and present the general results of computer simulation in Sec. III. In Sec. IV we concentrate on a special case and compare it with the FFM. Finally, a conclusion, together with a discussion on the application of our model, can be found in Sec. IV.

*Author to whom all correspondence should be addressed.

II. THE MODEL OF DIFFUSION AND DISSIPATION

We consider an $L \times L$ square lattice each of size $\Delta L \times \Delta L$. The energy contained in a lattice site $\mathbf{r}$ is denoted by $E(\mathbf{r})$, which is a non-negative real number. Since the sites are of equal areas, the ratio of the energy to the energy density is a constant for all sites. The evolution of the system is governed by the following rules.

(i) *Energy introduction.* At each time step, a unit amount of energy is added to a randomly selected site $\mathbf{r}_0$, i.e.,

$$E(\mathbf{r}_0) \rightarrow E(\mathbf{r}_0) + 1. \tag{1}$$

It should be noted that the energy introduction rate to the entire system is fixed. Our energy introduction rule takes only spatial fluctuation into account.

(ii) *Triggering of energy dissipation.* Whenever the energy of a site $\mathbf{r}_0$ reaches a fixed value E_{c1}, called the triggering threshold, energy stored at that site will be dissipated, i.e.,

$$\text{if } E(\mathbf{r}_0) \geq E_{c1}, \text{ then } E(\mathbf{r}_0) \rightarrow 0. \tag{2}$$

Note that the triggering threshold E_{c1} is the same at all sites and is time independent. The dissipation process is called "burning." Since all sites are of equal area, we can regard the "fire" as being triggered whenever the local energy density at some place exceeds a predetermined triggering threshold.

(iii) *Propagation of energy dissipation.* Nearest neighbors of a burning site burn provided their energy content is greater than or equal to a fixed value E_{c2} ($\leq E_{c1}$), called the propagation threshold, i.e.,

$$\text{if } E(\mathbf{r}_0') \geq E_{c2}, \text{ then } E(\mathbf{r}_0') \rightarrow 0 \tag{3}$$

whenever $\mathbf{r}_0'$ is a nearest neighbor of the burning site $\mathbf{r}_0$. We use periodic boundary conditions in the determination of neighboring sites. One may regard the triggering threshold E_{c1} as the (energy) density required to activate the dissipative process. Once the burning takes place, the energy release may heat up the neighboring sites and hence the density threshold required for the fire to propagate E_{c2} is reduced. This is valid in many physical and chemical reactions.

The burning process continues until no more lattice sites in the system catch fire. The energy dissipation (or outburst) is then completed. This is the fastest process in the system and so the whole burning process is assumed to take place in a single time step.

Finally, we define a "burnable cluster" as a collection of sites such that all of them will catch fire in case any single one of them burns. This is a useful concept when discussing the statistics of energy outburst.

(iv) *Energy diffusion.* Diffusion takes place in each time step, i.e.,

$$E(\mathbf{r}) \to E(\mathbf{r}) + \Delta E(\mathbf{r}) \quad \text{for all } \mathbf{r}, \tag{4}$$

where ΔE depends on the system configuration, the diffusion constant D, the lattice size ΔL, and the physical time Δt corresponding to a cellular automaton time step. But without lost of generality, we can always rescale our time and space to make both Δt and ΔL equal to 1. Furthermore, the method we use to evaluate $\Delta E(\mathbf{r})$ is reported in the Appendix.

Various initial conditions, such as those starting with all $E(\mathbf{r}) = 0$, have been used. However, the long term statistics is independent of the initial conditions because both burning and diffusion erase the history of the system. Although the model we have introduced is based on a two-dimensional square lattice, generalizations to other dimensions and griding methods are straightforward. A more complete study of the model in various dimensions is planned for future works [6]. Finally, a snapshot of a typical system configuration immediately before a fire is triggered is shown in Fig. 1.

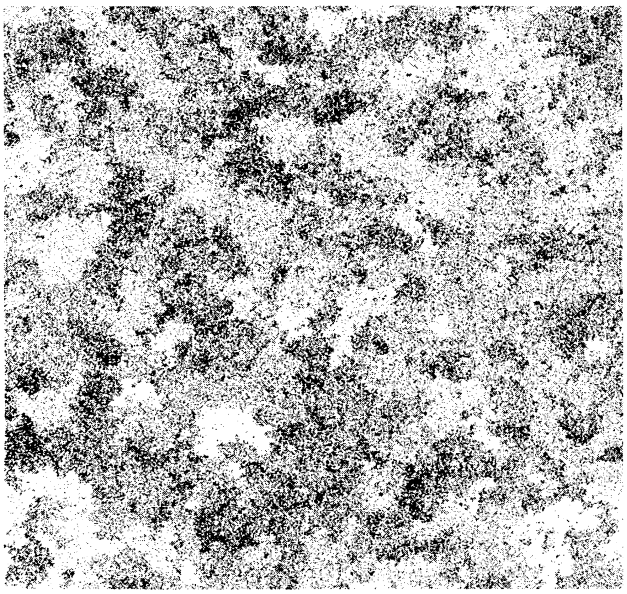

FIG. 1. Gray scale snapshot of a 512×512 lattice with $E_{c1} = 6$, $E_{c2} = 1$, and $D = 0$. The higher the value of E, the darker the dot.

III. EXPECTATIONS AND SIMULATION RESULTS

Before presenting the results of our numerical simulation, let us try to discuss qualitatively what we expect to see.

A. Expectations

There are three tuning parameters in our model, namely, E_{c1}, E_{c2}, and D. A large average dissipation size is a direct consequence of having large burnable clusters immediately before the system catches fire. Large burnable clusters can be obtained in either one of the following ways.

(i) *Large diffusion constant.* Diffusion spreads energy out and wipes out information on where the energy packet is first introduced to the system. Having a large D means that immediately before a sudden energy dissipation, the energy content in each site is approximately equal, except for those few sites where energy packets are recently introduced. So we expect the whole system to be covered by a single burnable cluster immediately before each burning.

(ii) *Small propagation to triggering thresholds ratio.* In this case, most of the sites have enough energy content to continue the propagation once the burning begins. Once again, we expect to find a single burnable cluster covering the entire system immediately before each burning [4].

Using the same argument, a small average dissipation size can be obtained when diffusion is unimportant and when E_{c2} is comparable to E_{c1}. For every fixed E_{c1} and E_{c2}, the average burnable cluster size immediately before a burning increases with D. Therefore, starting from a subcritical system (i.e., a system with small burnable clusters only) with $D = 0$, a supercritical system (i.e., a system with large burnable clusters only) can be obtained simply by increasing the value of D. We also expect to find a critical value of D, which is a function of E_{c1} and E_{c2}, such that burnable clusters of all sizes can be found immediately before burning. This is the critical state in our model. We have done numerical experiments confirming our expectations, which we will report in the following subsection.

B. Roles of diffusion

In order to study the effects of diffusion, we vary the diffusion constant D from 10^{-6} to 10^{-2} in a 64×64 lattice with E_{c1} and E_{c2} equal to 5.0 and 2.0, respectively. We found that the average size of energy dissipation $\langle S \rangle$ in-

creases as the diffusion constant D increases (see Fig. 2). Although we only report the system behavior when it assumes the above parameters, the general behavior of the system using different values of thresholds is unchanged.

We observe that when $D \gtrsim 3 \times 10^{-3}$, both the energy dissipation size S and the time since the last dissipation T become very regular (see Fig. 3). This is the consequence of having a single burnable cluster covering the whole surface just before the burning. Thus all the energy available in the system is dissipated during the burning. As a result, S equals the total amount of energy dumped into the system since its last dissipation, which is in turn equal to T. The strong correlation between S and T for a high diffusion system is shown in Fig. 4 (circle). To study this correlation, we define the correlation coefficient Γ by

$$\Gamma = \frac{\langle ST \rangle - \langle S \rangle \langle T \rangle}{\sigma_S \sigma_T}, \tag{5}$$

where σ_S and σ_T are the standard deviations of S and T, respectively. It can be shown that Γ varies from -1 to 1 and the value of 1 (-1) implies that S and T are completely positive (negative) correlated while 0 means that they are uncorrelated. The dashed line in Fig. 2 shows that Γ increases with increasing D, indicating a strong positive correlation between S and T for a system with a large diffusion constant. In this case, the distributions of the energy dissipation $P(S)$ and the time interval $P(T)$ are the same and both of them show localized skewed peaks (see Fig. 3).

For a smaller D $(5 \times 10^{-4} \lesssim D \lesssim 3 \times 10^{-3})$, the strong correlation between S and T begins to break down. Weaker diffusion permits greater fluctuation in the energy content at different sites. The system is likely to catch fire before all the sites are connected. Hence not all the energy available in the system is dissipated and some clusters may leave after a burning. As shown in Fig. 4, (S, T) (the plus symbols) are distributed around their mean values. In addition, if no burning is triggered for a sufficiently long time, a system-wide dissipation can happen. Γ decreases from 1 in this region as well. A consequence of the incomplete burning is that the probability of having a triggering site in a small burnable cluster is greatly increased. Events with a small energy dissipation begin to appear and hence the correlation Γ increases slightly as D decreases around $D = 6 \times 10^{-4}$.

As D decreases further $(10^{-5} \lesssim D \lesssim 5 \times 10^{-4})$, the small dissipation begins to dominate. In fact, $P(S)$ changes from a localized peak to a power law and finally to an exponential decay. In our simulation, we found that the critical diffusion constant D_{crit} to be 1.4×10^{-4}. Surely this critical value is a function of E_{c1} and E_{c2}. For even smaller D $(D < 10^{-5})$, diffusion becomes insignificant. The heights of nearby sites are nearly uncorrelated and hence $P(S)$ shows a very early cutoff (i.e., an exponential decay). Figure 3 depicts the localized skewed peak, power law, and exponential behaviors of $P(S)$ as a

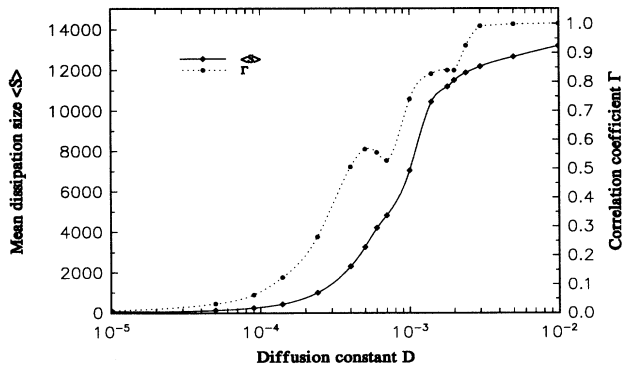

FIG. 2. Variation of the mean dissipation size $\langle S \rangle$ (solid line) and the correlation coefficient Γ (dashed line) against the diffusion constant D. All the simulations are done in a 64×64 lattice with $E_{c1} = 5.0$ and $E_{c2} = 2.0$, respectively. The same set of parameters is used in Figs. 3 and 4.

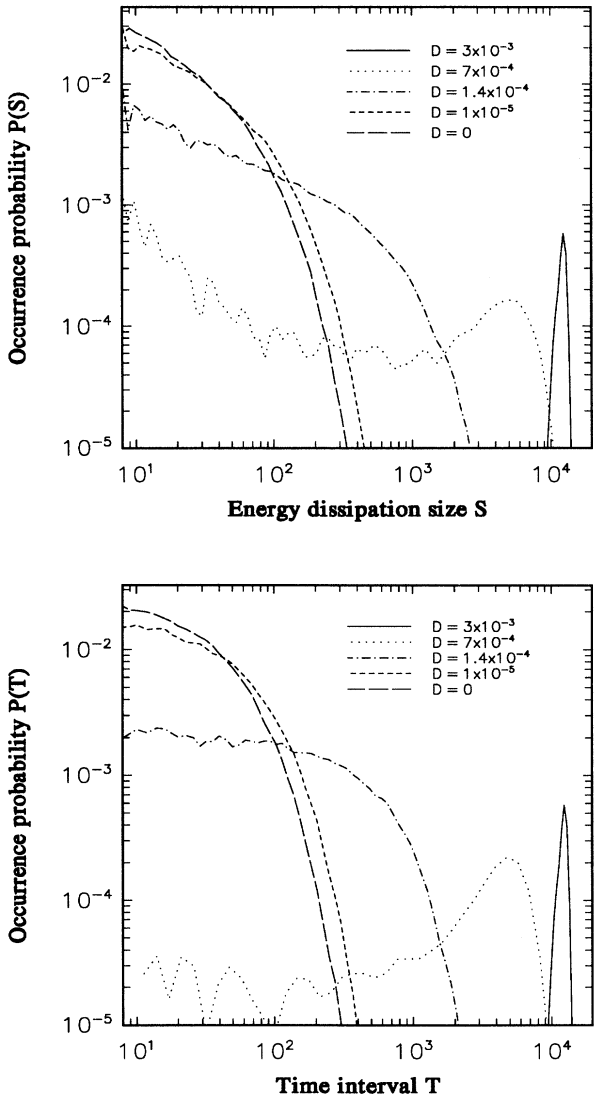

FIG. 3. Distributions of (a) the energy dissipation size S and (b) the time interval between successive energy dissipation T for different values of D.

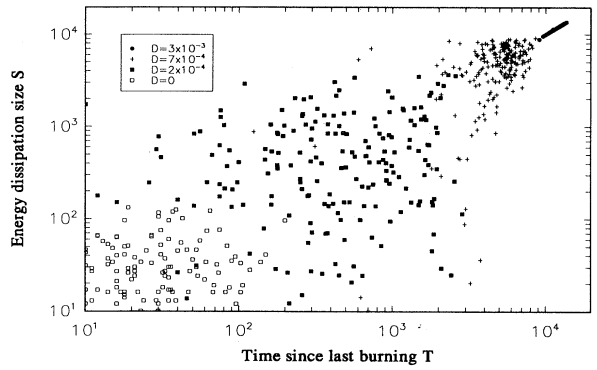

FIG. 4. Correlation of the time since the last energy dissipation T and the size of energy dissipation S for different values of D.

result of different diffusion constant D.

It should be noted that when $P(S)$ follows a power law, the corresponding distribution of the time interval between successive burning $P(T)$ decreases exponentially for large T. It means that there is a characteristic time interval for the occurrence of burnings even when scaling behavior is observed in the distribution of dissipation sizes. It is because the burnable clusters are spatially separated and the largest burnable cluster is only a portion of the system. The total number of critical sites in the entire system, and hence the probability of triggering a burning, is more or less the same all the time. It is expected that this case has similar features with respect to the one studied in Sec. IV.

C. Roles of triggering and propagation thresholds

In our simulations, we have not studied the effect of the thresholds on the model in detail. However, we believe that the above behaviors would be also observed when we vary E_{c1} or E_{c2} instead of D. In fact, when one of the three parameters is fixed, we may observe any one of the above behaviors by carefully choosing the other two parameters together with a reasonable lattice size. For example, reducing E_{c2} has similar effects as increasing D (see Fig. 5).

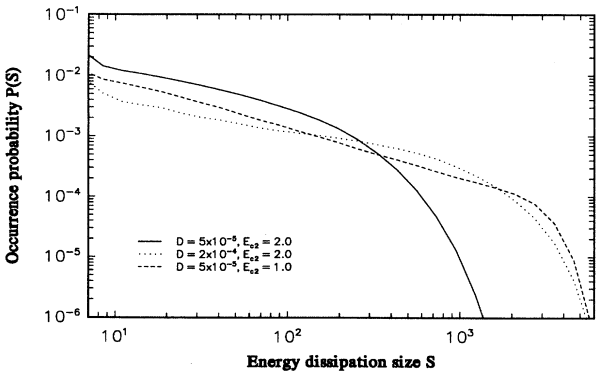

FIG. 5. Distribution of the energy dissipation size of a system with $D = 5 \times 10^{-5}$ and $E_{c2} = 2$ (solid line). The effect of increasing D to 2×10^{-4} (dotted line) is qualitatively similar to that of reducing E_{c2} to 1 (dashed line).

IV. COMPARISON WITH FOREST-FIRE MODEL

The forest-fire model was first introduced by Bak *et al.* as an example of self-organized criticality (SOC) [1]. They considered a lattice of cells where individual cell belongs to one of the following states: a green tree, a burning tree, or a void (i.e., no tree). In each time step, a tree grows on an empty cell with probability p and a green tree burns if at least one of its nearest neighbors contains a burning tree. Finally, a burning tree becomes a void in the next time step. Grassberger and Kantz [7] later showed that the model is not critical in the limit $p \to 0$. Later on, Drossel and Schwabl [8] modified the model by introducing a lightning probability f with which a green tree catches fire. This version of the FFM shows criticality in the sense that anomalous scaling laws are observed provided $(f/p)^{-\nu'} \ll p^{-1} \ll f^{-1}$, where $\nu' = 0.58$ for the two-dimensional FFM [9]. In this section we compare our model with the FFM introduced by Drossel and Schwabl.

The parameters of our model should be chosen reasonably so that our model would resemble the FFM. First of all, there is no diffusion in the FFM. So we require $D \ll 1$. The propagation of fire in the FFM is always allowed and thus we should have $E_{c2} \ll E_{c1}$. In the two-dimensional FFM, SOC behavior is claimed provided $(f/p)^{-0.58} \ll p^{-1} \ll f^{-1}$ [9]. It can be interpreted as the time taken by a forest fire is much shorter than the time taken by the growing of a tree, which is in turn much shorter than the time interval of two successive lightning occurrences at the same site. In our diffusive and dissipative cellular automaton model, the first criterion is satisfied automatically because it takes only one time step to burn down a cluster. For the second criterion, we should set $E_{c1} \gg 1$ in order to reduce the frequency of burning. On the other hand, E_{c1} should not be too large, or else the burnable clusters become too large and hence only large events are observed. This is consistent with the FFM in which f cannot be too small in comparison to p. After taking all the above criteria into consideration, we choose $E_{c1} = 6$, $E_{c2} = 1$, and $D = 0$ with a 512×512 periodic square lattice in our simulation. Of course, other choices of parameters are possible (e.g., $E_{c1} = 6$, $E_{c2} = 0.1$, and $D = 10^{-7}$) and the results obtained are qualitatively the same.

In the FFM, a cluster of size s is defined as a group of s neighboring sites with green trees. In contrast, the size s of a burnable cluster in our model is defined as the number of sites in that burnable cluster. In Fig. 6, we plot the distribution of cluster size $N(s)$ and the root mean quadratic radius $R(s)$. We find that

$$N(s) \sim s^{-\tau} \text{ with } \tau = 2.11 \pm 0.02 \tag{6}$$

and

$$R(s) \sim s^{1/\mu} \text{ with } \mu = 1.87 \pm 0.02. \quad (7)$$

While the exponent τ is similar to the accurate results obtained by Clar *et al.* [9] and Grassberger [10] for the FFM, the exponent μ differs from the numerical value of 1.96 ± 0.01 obtained recently by Clar *et al.* in their FFM simulations [9].

We then study the model with different E_{c1} and some numerical results are tabulated in Table I. The mean density ρ of sites with energy content greater than the propagation threshold E_{c2} can be related to the average burning size $\langle S \rangle$ by

$$\langle S \rangle \sim |\rho_c - \rho|^{-\gamma}, \quad (8)$$

where ρ_c is the mean density at the critical point. Using the measured results we have estimated that

TABLE I. Numerical results on a 512×512 lattice with $E_{c2} = 1$ and $D = 0$.

E_{c1}	Γ	$\langle E \rangle$	ρ
4	-0.011 ± 0.006	53.0 ± 0.4	0.3343 ± 0.0005
5	-0.008 ± 0.006	178 ± 2	0.363 ± 0.001
6	$+0.012 \pm 0.006$	643 ± 6	0.381 ± 0.001
7	$+0.02 \pm 0.01$	2440 ± 40	0.393 ± 0.001

$$\rho_c = 0.410 \pm 0.002, \quad (9)$$

$$\gamma = 2.57 \pm 0.01. \quad (10)$$

Although the fitted value of γ is different, ρ_c is the same as that of the FFM within numerical accuracy.

The greatest difference between our model and the FFM is the probability $p(s)$ of burning for a cluster of

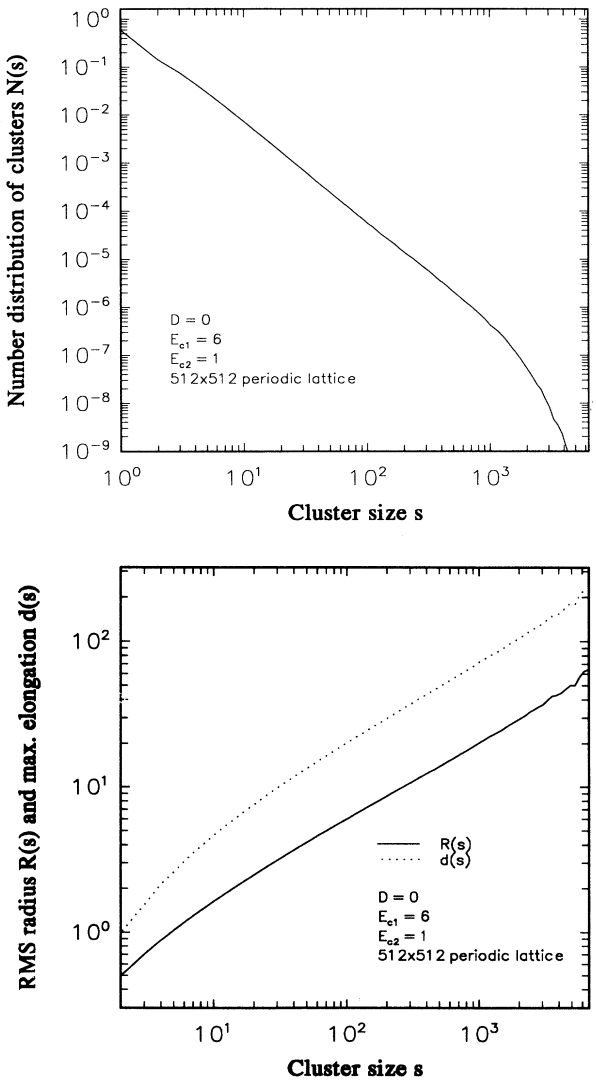

FIG. 6. Distribution of (a) cluster size $N(s)$; (b) rms radius $R(s)$ and maximum elongation $d(s)$.

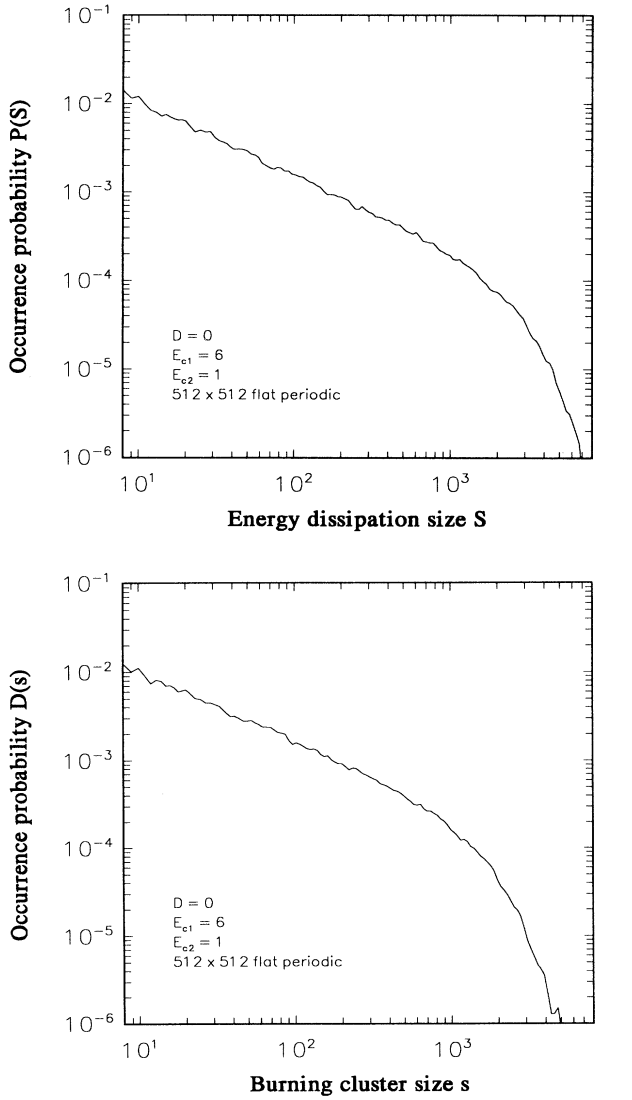

FIG. 7. Plot of (a) $P(S)$ against S and (b) $D(s)$ against s with $E_{c1} = 6$, $E_{c2} = 1$, and $D = 0$ in a 512×512 lattice. A scaling region from 10 to 10^3 is observed with an exponent of -0.85.

size s. In the FFM, $p(s)$ is proportional to s as all cluster sites are triggering sites in the sense that they are ready to trigger a fire once lightning occurs. But in our model only a small percentage of the sites in a burnable cluster are triggering sites. Figure 7 shows that the distribution of the energy dissipation $P(S)$ scales as $S^{-\alpha}$ with an $\exp(-S/S_\xi)$ cutoff. We also plot the distribution of burning cluster size $D(s)$ and find that within the accuracy of our simulation, $P(S)$ and $D(s)$ share the same exponent in the scaling region. Thus we have $s \sim S$ and hence

$$D(s) \propto s^{-\alpha} \exp(-s/s_\xi) \text{ with } \alpha = 0.85 \pm 0.01, \quad (11)$$

while it is known that $\alpha \approx 1.0$ for the FFM. Further numerical experiments show that α decreases as D increases in our model (see Fig. 5). In conclusion, although our model is similar to the FFM, they belong to two different universality classes.

Although α depends on the value of D, we find, within numerical errors, that the value of α does not change with E_{c1}. In Fig. 8 one can see that different E_{c1} affects the range of scaling region but not the scaling exponent of $P(S)$. It is easy to realize that for a larger E_{c1} it takes a longer time to trigger a burning and allows the growth of larger clusters. In order to prove that the falloff of $D(s)$ for large s is not due to the finite size of the system, simulations using a larger lattice size have been done and the same spectra of $D(s)$ (in terms of the number of sites s) are obtained. Furthermore, the distribution of time interval between successive burnings $P(T)$ shows an exponential decay as discussed in Sec. II. We conclude in our simulation that no system-wide dissipation occurs.

In addition to the rms radius, we define a maximum elongation $d(s)$, which is the maximum distance between any two sites in a cluster of size s, to investigate the shape of the clusters. We found that

$$d(s) \sim s^{1/\mu'} \text{ with } \mu' = 1.82 \pm 0.02. \quad (12)$$

Figure 6(b) tells us that for small s, both $R(s)$ and $d(s)$ deviate from a straight line. This is because of the discreteness of the lattice. For a larger value of s, however, they follow power laws of similar exponents and the ratio $d(s)/R(s)$ increases to a constant value around 2.8, which is very close to the value of a two-dimensional compact circular object (which equals $\sqrt{8}$). This concludes that small burnable clusters are generally irregular and asymmetric objects due to the random fluctuation of their formation. As the size of a burnable cluster increases, clusters become more and more regular and spherical. The ratio $d(s)/R(s)$ shows that, on the average, the clusters are more or less compact objects for large s. On the other hand, the values of μ and μ' suggest that the clusters may have fractal structures with a dimension around 1.9. However, at this stage we cannot determine the fractal dimension with accuracy because there is no general efficient method to estimate it and also our simulation is not close enough to the critical point of the system. It is interesting to note that when we choose a random site near the center of mass of a large cluster, the average local density of the cluster around that site is close to the site percolation threshold 0.59. We believe that there is a close relationship between site percolation and our model (or the FFM) and further investigation is needed to draw any conclusion.

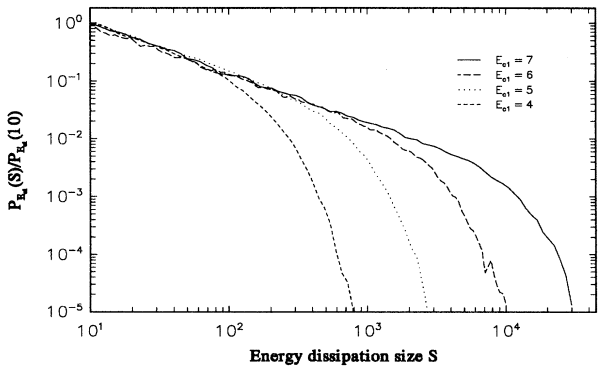

FIG. 8. Distribution of the energy dissipation size $P(S)$ with E_{c1} =7 (solid line), 6 (long-dashed line), 5 (dotted line) and 4 (medium-dashed line) for a 512×512 lattice. $E_{c2} = 1$ and $D = 0$. As in the S vs $P_{E_{c1}}(S)/P_{E_{c1}}(10)$ plot, the scaling region increases with increasing E_{c1}. However, the scaling exponent is independent of E_{c1}.

V. CONCLUSIONS AND OUTLOOK

In this paper, we introduce a cellular automaton model for diffusive and dissipative systems and described its behaviors in different locations in parameter space. First, we study the effect of diffusion and find that $P(S)$ may follow a localized skewed peak, power law, or exponential decay. Then we consider the case without diffusion and compare it with the famous forest-fire model.

With a careful choice of parameters and geometry, this model is able to describe qualitatively the behavior of a number of physical systems, including the behaviors of type-I x-ray bursters (details can be found in Ref. [4]) and CO_2 gas outbursts in some crater lakes (details can be found in Ref. [5]). The following is a brief description of the above two physical systems and the reason why our cellular automaton model can be used to describe their behaviors.

Type-I x-ray bursts are results of thermonuclear explosions on the surface of an accreting neutron star. Nuclear fuel, usually making up of hydrogen and helium, is deposited on the neutron star surface. Whenever the local density of nuclear fuel is greater than a threshold value, which is determined by the specific nuclear reaction involved, a thermonuclear runaway takes place. The nuclear reaction can spread to its neighbors if they contain a sufficient amount of nuclear fuel. It results in a transient flash in the x-ray band, called a type-I x-ray burst. Type-I bursts are different from the more frequently repeating type-II bursts, which are believed to be results of accretion disk instability [11]. It is easy to estimate also that the material diffusion time scale in this problem is long compared to the typical time interval between two successive bursts. Thus material diffusion is not im-

portant in this problem. After taking into account the spatial fluctuation in the accretion process, the system can be described using our cellular automaton model on a spherical surface with $D = 0$. In addition, the values of E_{c1} and E_{c2} can be determined in principle once the specific nuclear reaction, cooling process, and the typical mass of an accreting blob are given. The burst statistics predicted by our model is consistent with observations [4].

Another application of the diffusive and dissipative model is the gas outburst statistics in some crater lakes. CO_2 gas is injected to the bottom of the lake by some natural processes [12]. Note that the solubility of CO_2 in water increases with pressure (and hence the depth of water). So once the CO_2 concentration in the bottom of the lake becomes supersaturated, gas bubbles will form and it will drive the water around it to move up causing further degassing. A catastrophic gas outburst results. Taking into account the horizontal water flow in the lake, we can describe the outburst of a crater lake using our model with a large D and hence a rather regular gas outburst is expected.

Further investigation of this model in other spatial dimensions, the behavior of the model at criticality as a function of the diffusion constant D, and other possible applications of the model are planned to be reported in future work [6].

ACKNOWLEDGMENTS

We would like to thank B. Drossel for useful comments. This work is supported by a UPGC grant of Hong Hong, DOE Grant No. DE-FG02-90ER40542, and NSF Grant No. AST-9315133.

APPENDIX: METHOD OF HANDLING DIFFUSION

The energy diffusion equation in continuous flat two-dimensional space is

$$\frac{\partial \rho}{\partial t} = D\left(\frac{\partial^2 \rho}{\partial x^2} + \frac{\partial^2 \rho}{\partial y^2}\right), \tag{A1}$$

where ρ is the energy density. In our cellular automaton model, we approximate the above equation using the finite difference

$$E(\mathbf{r}, t + \Delta t) = D\frac{\Delta t}{\Delta L^2}\sum_{\mathbf{r}'}[E(\mathbf{r}', t) - E(\mathbf{r}, t)] + E(\mathbf{r}, t)$$

$$\text{for all } \mathbf{r}, \tag{A2}$$

where $E(\mathbf{r}, t)$ is the energy content of site $\mathbf{r}$ are time t and the sum is over all the nearest neighbors of $\mathbf{r}$. This is possible since the areas of lattice sites are the same. The value of D is coupled with the system size and the time step employed. Equation (A2) is a good approximation to the actual diffusion process in continuous space-time if $D\Delta t/\Delta L^2 \ll 1$. This criterion is satisfied in all the cases we have reported in this paper. In the event that D is too large, an adaptive integration scheme to calculate $E(r, t + \Delta t)$ is employed.

The diffusion constant is an invariant under any rescaling of the system. This is true provided the changes in ΔL and Δt are correlated, that is, $\Delta t \longrightarrow \lambda^2 \Delta t$ whenever $\Delta L \longrightarrow \lambda \Delta L$.

[1] P. Bak, K. Chen, and C. Tang, Phys. Lett. A **147**, 297 (1990).
[2] M. Eden, in *Proceedings of the Fourth Berkeley Symposium on Mathematical Statistics and Probability*, edited by F. Neyman (University of California Press, Berkeley, 1961), Vol. 4.
[3] P. Bak and C. Tang, J. Geophys. Res. B **94**, 15 635 (1989); K. Christensen and Z. Olami, Phys. Rev. A **46**, 1829 (1992).
[4] H. F. Chau, K. S. Cheng, T. C. Chan, and F. K. Lamb, Astrophys. J. (to be published).
[5] H. F. Chau, P. K. Kwok, and L. Mak (unpublished).
[6] T. C. Chan, H. F. Chau, and K. S. Cheng (unpublished).
[7] P. Grassberger and H. Kantz, J. Stat. Phys. **63**, 685 (1991).
[8] B. Drossel and F. Schwabl, Phys. Rev. Lett. **69**, 1629 (1992).
[9] S. Clar, B. Drossel, and F. Schwabl, Phys. Rev. E **50**, 1009 (1994).
[10] P. Grassberger, J. Phys. A **26**, 2081 (1993).
[11] W. H. G. Lewin, J. Van Paradijs, and R. E. Taam, Space Sci. Rev. **62**, 223 (1993), and references cited therein.
[12] G. W. Kling *et al.*, Science **236**, 169 (1987), and references cited therein.